Journal of Structural Geology 33 (2011) 1325–1333

Contents lists available at ScienceDirect

Journal of Structural Geology

journal homepage: www.elsevier.com/locate/jsg

A new macroscopic method of fabric analysis based upon Fresnel's theorem

Yehua Shan [a,b,*], Wenjiao Xiao [c]

[a] Laboratory of Marginal Sea Geology, Guangzhou Institute of Geochemistry, Chinese Academy of Sciences, Guangzhou City 510640, PR China
[b] Xinjiang Research Centre for Mineral Resources, Xinjiang Institute of Ecology and Geography, Chinese Academy of Sciences, Urumqi 830011, PR China
[c] State Key Laboratory of Lithospheric Evolution, Institute of Geology and Geophysics, Chinese Academy of Sciences, Beijing City 100029, PR China

ARTICLE INFO

Article history:
Received 29 November 2010
Received in revised form
1 June 2011
Accepted 28 June 2011
Available online 3 July 2011

Keywords:
Fresnel's theorem
Fabric analysis
Stress
Strain
Equivalence

ABSTRACT

Fresnel's theorem used in optical crystallography is applicable to fabric analysis, strain analysis and stress analysis due to the similarity in formulation between the optical indicatrix, the fabric ellipsoid, the strain ellipsoid and the stress ellipsoid. It describes the relationship between the fabric trace on any section and the circular sections of the fabric ellipsoid. Its explicit expression is equivalent to the expression of the Wallace-Bott hypothesis for stress inversion. A new method is thus developed in this paper to determine the fabric ellipsoid from no less than four independent sectional measurements. Artificial and real examples are taken to illustrate the feasibility of this new method. The advantage of the method over some of the existing graphic methods is that it can deal with any set of sectional measurements.

1. Introduction

Determining the strain in rock is of practical use in quantifying the plastic deformation that the rock has undergone. Normally, strain markers are first measured on several differently-oriented section planes to estimate sectional strain ellipses. Assuming the strain to be homogeneous on the scale of the outcrop, these strain ellipses are then used in some way to determine the strain ellipsoid. Numerous methods of strain analysis (Ramsay, 1967; Ramsay and Huber, 1983) have been developed for the first of these steps, but this paper only concerns the second step. There are two categories of procedure for determining the strain ellipsoid from the sectional strain ellipses, numerical (e.g. Shimamoto and Ikeda, 1976; Oertel, 1978; Milton, 1980; Gendzwill and Stauffer, 1981; Owens, 1984; Shao and Wang, 1984; Wheeler, 1989; De Paor, 1990; Robin, 2002; Shan, 2008; Shan et al., 2008) and graphic (Ramsay, 1967; Lisle, 1976). A majority of methods in the former category differ in the way of tackling the consistency of the strain ellipses on the sections, and the latter category includes the distribution of elongation and the Tocher's (1964) crystallographic method (Lisle, 1976). It is worthy to note that, some or all of these various methods are also applicable to theoretically similar fabrics in other disciplines, for example, the optical crystallography (Shubnikov, 1960) and paleomagnetism (Lanza and Meloni, 2006).

In spite of the close relationship between strain and stress, nearly all existing methods of inverting the stress from fault/slip data measured in the field (see the brief reviews of Nemcok and Lisle, 1995; Shan et al., 2003; and Zalohar and Vrabec, 2007) appear to have nothing to do with the strain methods mentioned above. They are based upon the Wallace-Bott hypothesis that assumes the parallelism between the resolved shear stress on the fault plane and the observed slip line on it. However, Shan and Li (2008) recently found a similarity in formulation between the equation describing the sectional strain ellipse and the equation describing the hypothesis for a given fault/slip datum. In this sense, the stress may be estimated using one of the strain methods if the fault/slip data are transformed into corresponding sectional measurements; or vice versa. For example, they use the Tocher's (1964) graphical method to determine on the stereogram the stress from measured fault/slip data.

Following the study of Shan and Li (2008), this short communication further addresses the similarity between strain analysis and palaeostress analysis. As shown below, Fresnel's theorem (see Shubnikov, 1960, p.70) can be described by an explicit equation that is identical in formulation to the equation of the Wallace-Bott hypothesis. This similarity permits the use of the moment method (Fry, 1999; Shan et al., 2003) in solving a set of such over-determined equations for the strain ellipsoid, and simplifies the conversion between sectional measurements of strain ellipses and fault/slip data.

The definitions of symbols used in this paper are listed in Table 1.

* Corresponding author. Guangzhou Institute of Geochemistry, Laboratory of Marginal Sea Geology, Wushan, Guangzhou, Guangdong 510064, China. Tel.: +86 20 85292403; fax: +86 20 85290130.
E-mail address: shanyehua@yahoo.com.cn (Y. Shan).

0191-8141/$ – see front matter © 2011 Elsevier Ltd. All rights reserved.
doi:10.1016/j.jsg.2011.06.009

Table 1
The definitions of symbols used in the paper.

Symbols	Definitions	Comments
O_j	Pole to the circular section of the fabric ellipsoid	$j = 1, 2$; Figs. 1 and A1; Eqs. (A23) and (A24)
F	Pole to an exposure or section	Fig. 1
S	fabric trace	Fig. 1
P	$P = F \times S$	Fig. 1b
R_j	$R_1 = F \times O_1$, and $R_2 = F \times O_2$	$j = 1, 2$; Fig. 1b
R'_j	$R'_1 = R_1/\|\|R_1\|\|$, and $R'_2 = R_2/\|\|R_2\|\|$	$j = 1, 2$; Fig. 1b
P_j	Projections toward line FP of R_1 and R_2	$j = 1, 2$; Fig. 1b
$\|\|\|$	Length of a vector	
$\overline{AB}$	Euclidean distance between points A and B	
$A \cdot B$	Dot product of vectors A and B	
o_{ji}	The i-th component of the pole to the j-th circular section	$i = 1, 2, 3$; $j = 1, 2$; Eqs. (9), (11), (12), (A1), (A3)–(A17), (A19), (A20), (A25), (A26), and (A29)
s_i	The i-th component of vector S	$i = 1, 2, 3$; Eqs. (9), (11), (12)
p_i	The i-th component of vector P	$i = 1, 2, 3$; Eqs. (9), (11), (12)
n_i	The i-th component of the normal to a fault plane	$i = 1, 2, 3$; Eq. (13)
l_i	The i-th component of the vector perpendicular to the slip line on the fault plane	$i = 1, 2, 3$; Eq. (13)
σ_{ij}	The component of the stress	$\sigma_{ij} = \sigma_{ji}$, $i,j = 1, 2, 3$; Eq. (13)
ϵ_i	The square of the lengths of the X-, Y- and Z-coordinate axes of the fabric ellipsoid for $i = 1$, 2, and 3, respectively	$i = 1, 2, 3$; Eqs. (A1), (A6), (A7), and (A18)–(A30)
k and t	Unknown constants	Eqs. (A6), (A7), (A18)–A(22), and (A27)–(A30)
V	Acute angle between either O_1 or O_2 and the long axis of the fabric ellipsoid	Fig. A1; Eqs. (A25), (A26)
ε_{max},ε_{int} and ε_{min}	The long, intermediate and short axes of the fabric ellipsoid	Fig. A1

2. Fresnel's theorem

In optical crystallography, the directions of extinction on sections of different orientation are controlled by the character of the optical indicatrix. Here we consider the common case of an indicatrix with the shape of a triaxial ellipsoid where there exist two circular sections, O_1 and O_2. In this case, the indicatrix is well defined by the locations of the circular sections. Fresnel's theorem states that (see Shubnikov, 1960, p.70), for a given exposure (section) plane with a pole F and a fabric trace S on the exposure plane, the angle between planes FO_1 and FO_2 is bisected by plane FS (Fig. 1a), or

$$\angle SFO_1 = \angle SFO_2 \tag{1}$$

This highlights a way of determining the optical indicatrix by looking on the stereogram at the sides of plane FS for the areas where O_1 and O_2 are located. Tocher (1964) developed a simple graphic method that reduces the area of the greater side by subtracting from it a part symmetrical to the smaller side along the trend of the great circle containing points F and S. As the optical indicatrix is analogous to the strain ellipsoid, this method was later applied to strain analysis (Lisle, 1976), and even to paleostress analysis (Shan and Li, 2008).

In the light of the poles to the planes in Fig. 1a, Eq. (1) is rewritten as

$$\angle PFR'_1 = \angle PFR'_2 \tag{2}$$

or

$$\overline{PR'_1} = \overline{PR'_2} \tag{3}$$

where P, R'_1 and R'_2 are poles of planes FS, FO_1 and FO_2 (Fig. 1b), respectively, and $\overline{PR'_1}$ is the Euclidean distance between points P and R'_i ($i = 1$ or 2). $P = F \times S$, $R'_1 = R_1/\|R_1\|$, $R'_2 = R_2/\|R_2\|$, $R_1 = F \times O_1$, and $R_2 = F \times O_2$, where $\|\|$ is the length of a vector.

Because R'_1 and R'_1 lie at the sides of a plane normal to S, their dot products with the normal have similar value but different sign.

$$S \cdot R'_1 = -S \cdot R'_2 \tag{4}$$

$$S \cdot \frac{R_1}{\|R_1\|} = -S \cdot \frac{R_2}{\|R_2\|} \tag{5}$$

$$\frac{S \cdot R_1}{S \cdot R_2} = -\frac{\|R_1\|}{\|R_2\|} \tag{6}$$

Let P_1 and P_2 stand for points where R_1 and R_2 are projected toward line FP. Obviously, $\Delta FPR'_1 \cong \Delta FPR'_2$, $\Delta FP_1R_1 \approx \Delta FP_2R_2$. Therefore,

$$\frac{\|R_1\|}{\|R_2\|} = \frac{\overline{FP_1}}{\overline{FP_2}} = \frac{P \cdot R_1}{P \cdot R_2} \tag{7}$$

where $\overline{FP_i}$ is the Euclidean distance between points F and P_i ($i = 1$ or 2).

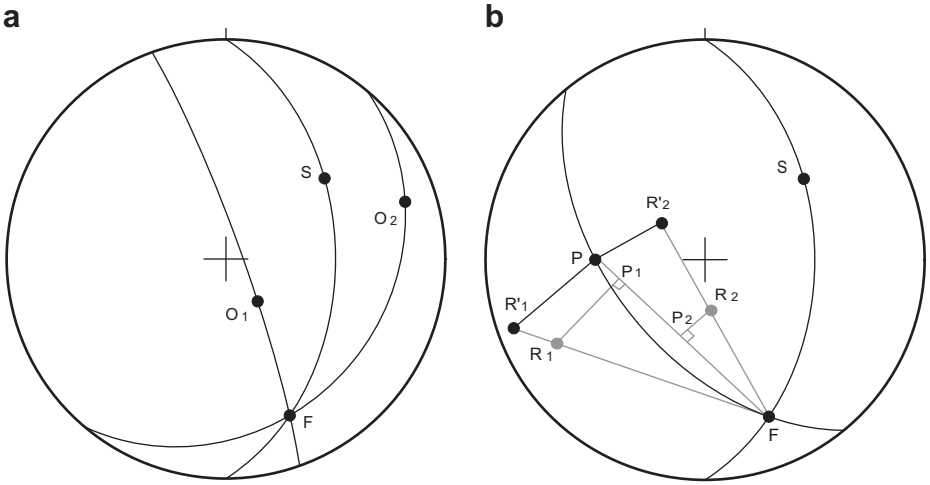

Fig. 1. According to Fresnel's theorem, on the stereogram (a) plane FS bisects the angle between planes FO_1 and FO_2, or $\angle SFO_1 = \angle SFO_2$, where F is the pole to a sectional measurement, S is the fabric trace on the section, and O_1 and O_2 are the poles to the circular sections of the fabric ellipsoid, and (b) $\angle PFR'_1 = \angle PFR'_2$, where P, R'_1 and R'_2 are poles of planes FS, FO_1 and FO_2. $P = F \times S$, $R'_1 = R_1/\|R_1\|$, $R'_2 = R_2/\|R_2\|$, $R_1 = F \times O_1$, and $R_2 = F \times O_2$, where $\|\|$ is the length of a vector. $\Delta PFR'_1 \cong \Delta PFR'_2$, and $\Delta PFR_1 \approx \Delta PFR_2$.

Substituting Eq. (7) into Eq. (6) gives

$$\frac{S\cdot R_1}{S\cdot R_2} = -\frac{P\cdot R_1}{P\cdot R_2} \tag{8}$$

Let $O_1 = [o_{11}\ \ o_{12}\ \ o_{13}]$, $O_2 = [o_{21}\ \ o_{22}\ \ o_{23}]$, $S = [s_1\ \ s_2\ \ s_3]$ and $P = [p_1\ \ p_2\ \ p_3]$. After rewriting Eq. (8) in terms of vector components, we have the following expression,

$$\begin{aligned} &2s_1p_1o_{11}o_{21} + 2s_2p_2o_{12}o_{22} + 2s_3p_3o_{13}o_{23} + (s_1p_2 + s_2p_1) \\ &\times (o_{11}o_{22} + o_{12}o_{21}) + (s_1p_3 + s_3p_1)(o_{11}o_{23} + o_{13}o_{21}) \\ &+(s_1p_3 + s_2p_3)(o_{12}o_{23} + o_{13}o_{22}) = 0 \end{aligned} \tag{9}$$

Among the six composite variables on the left-hand side, the first three are dependent because, as previously defined (Fig. 1b), vectors P and S are mutually perpendicular.

$$s_1p_1 + s_2p_2 + s_3p_3 = 0 \tag{10}$$

Solving s_3p_3 from Eq. (10) and inserting it into Eq. (9) leads to,

$$\begin{aligned} &2s_1p_1(o_{11}o_{21} - o_{13}o_{23}) + 2s_2p_2(o_{12}o_{22} - o_{13}o_{23}) \\ &+(s_1p_2 + s_2p_1)(o_{11}o_{22} + o_{12}o_{21}) + (s_1p_3 + s_3p_1) \\ &(o_{11}o_{23} + o_{13}o_{21}) + (s_1p_3 + s_2p_3)(o_{12}o_{23} + o_{13}o_{22}) \\ &= 0 \end{aligned} \tag{11}$$

This algebraic equation describes Fresnel's theorem in terms of the poles to the circular sections of the fabric ellipsoid, O_1 and O_2. As the bearings and plunges of the poles are unknown, a minimal number of four independent exposures are required to solve in some way such equations for them, under the constraint of unit length of the poles. Once their orientations are obtained, the directions and relative magnitudes of the major axes of the corresponding ellipses are readily determined from them (Lisle, 1976; see the Appendix). However, the way to the direct solution to Eq. (11) is complicated due to the nonlinearity.

3. Comparison

Rewriting Eq. (9) in matrix form,

$$[s_1\ \ s_2\ \ s_3]\begin{bmatrix} 2o_{11}o_{21} & o_{11}o_{22}+o_{12}o_{21} & o_{11}o_{23}+o_{13}o_{21} \\ & 2o_{12}o_{22} & o_{12}o_3^2+o_{13}^1o_{22} \\ \text{symmetrical} & & 2o_{13}o_{23} \end{bmatrix} \times \begin{bmatrix} p_1 \\ p_2 \\ p_3 \end{bmatrix} = 0 \tag{12}$$

As shown in the Appendix, the relative fabric ellipsoid (Shan and Li, 2008) is described by the middle matrix on the left-hand side, from which we know only the principal directions and the shape of the ellipsoid.

On the other hand, the most important assumption for stress inversion is the Wallace-Bott hypothesis that the resolved shear stress on the fault plane is parallel to the observed slip line on the plane (Carey and Brunier, 1974),

$$[n_1\ \ n_2\ \ n_3]\begin{bmatrix} \sigma_{11} & \sigma_{12} & \sigma_{13} \\ \sigma_{21} & \sigma_{22} & \sigma_{23} \\ \sigma_{31} & \sigma_{32} & \sigma_{33} \end{bmatrix}\begin{bmatrix} l_1 \\ l_2 \\ l_3 \end{bmatrix} = 0 \tag{13}$$

where n_i is the component of the normal to a fault plane, l_i is the component of the vector perpendicular to the slip line on the fault plane, and σ_{ij} is the components of the stress ($i,j = 1,2,3$). $\sigma_{ij} = \sigma_{ij}$. For a group of no less than four fault/slip data of a single tectonic phase, a set of such equations determined or over-determined are solved simultaneously in some way for the reduced stress, including the principal directions and Bishop's (1966) stress ratio.

Comparing Eq. (12) with Eq. (13) reveals no difference between them. For both equations, on the left-hand side the two vectors, the first and third matrixes, are mutually perpendicular and the middle matrix is symmetrical. This demonstrates the similarity in formulation between fabric analysis and stress inversion. This further inspires us to solve for the positions of O_1 and O_2 in a simpler way that uses the moment method (Fry, 1999; Shan et al., 2003) to determine the relative strain ellipsoid, and then calculates the orientations of the circular sections from the known ellipsoid. Fry (1999) and Shan et al. (2003) give detailed description about the moment method.

4. Procedure

The above-mentioned method for determining the circular sections of the fabric ellipsoid is implemented as follows:

1) Based upon the fabric measurements including the orientations of the sections (F) and the fabric traces (S) on the sections, calculate point P, according to $P = F \times S$.
2) In a way similar to that for processing the fault/slip data (Fry, 1999; Shan et al., 2003), vectors P and S are used to calculate the datum vectors in parameter space, from which the data matrix is made.
3) Use the moment method (Fry, 1999; Shan et al., 2003) to solve for the relative fabric ellipsoid that corresponds to the eigen vector in respect to the least eigen value of the data matrix. Once a solution to the relative ellipsoid is obtained, its negative is another possible solution. Discriminating between the two choices requires the consideration of the orientations of the observed fabric traces in relation to the calculated ones. The fit percentage is defined as the percent of sectional measurements where the acute angles between the observed trace and the calculated trace on the section are less than 45°. Only the solution having a fit percentage of 100% is accepted with confidence; otherwise, it is discarded.
4) Determine the eigen vectors and eigen of the relative fabric ellipsoid by use of the Jacobi method (see Shan et al., 2003, 2008). The eigen vectors in order of an increasing eigen value corresponds to the principal directions of the long, intermediate and short axes of the fabric ellipsoid, respectively, and the eigen values are used to calculate the acute angle (V) between O_1/O_2 and the long axes, a measure of the shape of the fabric ellipsoid (Lisle, 1976; see the Appendix).
5) Calculate the orientations of circular sections from the principal directions and angle V that are determined in the previous step (see the Appendix).

5. Tests using artificial examples

In order to show the feasibility of the above-proposed method, artificial examples are chosen in this section. A set of four independent artificial measurements (Fig. 2) is first generated at random under the prescribed fabric ellipsoid where the long axis is directed upwards, the short axis is directed toward the east, and V is 46.58°. The set has no measurement error. Then, a certain measurement area is added to the bearings of the fabric traces, and their plunges are recalculated so that the considered traces lie in the sectional planes. There are two choices for combining the error, addition and subtraction, for each individual sectional measurement; hence, we have an ensemble of 2^4 sets having a certain amount of measurement error. The measurement error is assigned with a value having a range of 0–10° in increments of 0.5°. Figs. 3 and 4 show results from applying the proposed methods to these numerous sets.

In Fig. 3, the calculated fabric ellipsoid from the primary set matches the prescribed fabric ellipsoid very well. When the

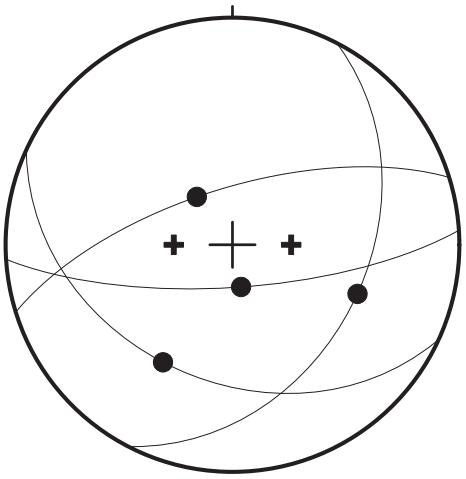

Fig. 2. Lower-hemisphere, equal-area projection of an artificial set of four measurements without any measurement error. The great circle represents the plane that contains the fabric trace shown in dot and the pole to the section, and the plus symbol marks the poles to the circular sections of the fabric ellipsoid obtained using the proposed method.

measurement error is taken into consideration, there appears a chance of having mismatch between the two ellipsoids. The mismatch strongly tends to increase with the amount of the measurement error. What is worse, if the mismatch is sufficiently large, there may exist at least one of 2^4 sets with a certain measurement error, whose calculated fabric ellipsoid never fits all of the fabric traces or has a fit percentage of less than 100%. This appears to happen only if the measurement error is larger than 3.5° (Fig. 4).

6. Applications

Three real examples taken from (Lisle, 1976; Table 2) are measurements on the cozonal sections i.e., a set of section planes that share a common axis. They represent a case of strong foliation and weak lineation, very weak foliation and weak lineation, and weak foliation and strong lineation, respectively (Lisle, 1976). Applying the proposed method to them gives rise to results shown in Fig. 5 and listed on Tables 2, 3. For comparison, the estimated fabric ellipsoids using the Tocher's (1964) method (Lisle, 1976) are also listed on Table 2.

6.1. Set one

For this set, the calculated fabric ellipsoid by our method badly matches the estimated fabric ellipsoid by the Tocher's method, although they both have an almost vertical dip angle of the foliation (Table 2). For the former, the first measurement appears odd in that its measured trace is almost perpendicular to the calculated trace on the sectional plane (Fig. 5a–b).

Table 3 lists the eigen values of data matrix for the set. The least eigen value is zero because the set has a minimal number of 4. The second least eigen value is about 0.01, much smaller than the third least eigen value, 0.84. This most probably suggests the dependency of the measurements in the set that fails to define a hyperplane in parameter space, to which the normal is the sole solution we look for (Shan and Fry, 2006). Were it true there would exist an infinite number of acceptable solutions, instead, that can be determined using the method by Shan and Fry (2006).

Fig. 6 displays the range of the poles to the circular sections of all acceptable ellipsoids. Approximately in the range lie the poles to the circular sections of the estimated ellipsoid using the Tocher's

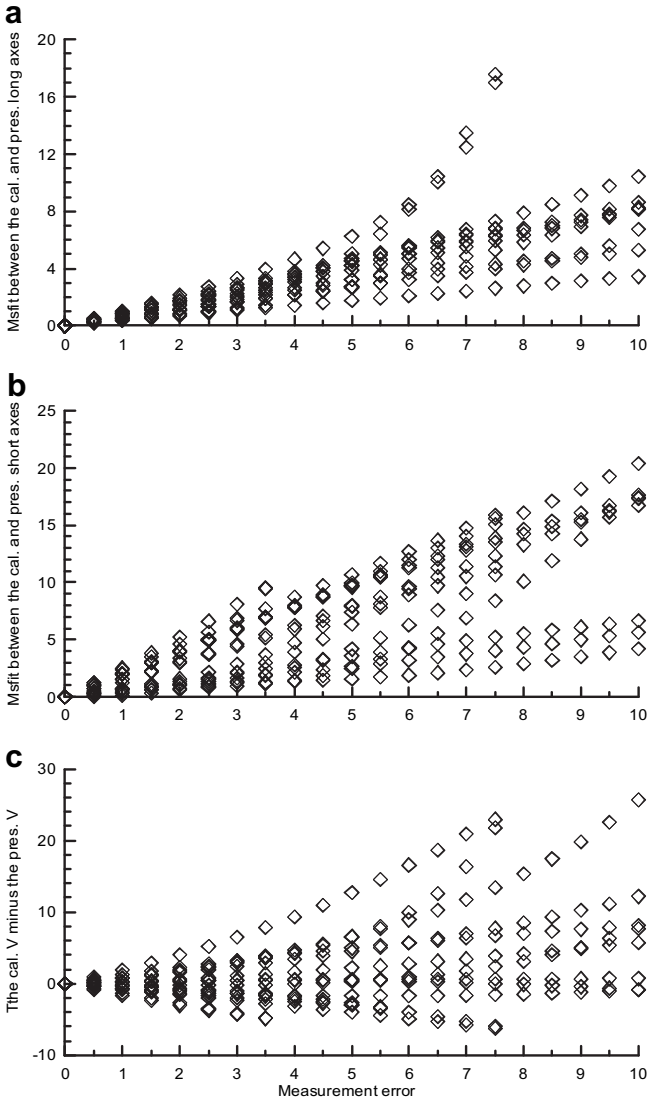

Fig. 3. Comparison of the prescribed fabric ellipsoid with the calculated fabric ellipsoids from artificial sets with a measurement error of 0–10°. (a)–(c) is for the long axis, the short axis, and the acute angle (V) between the long axis and one of the poles to the circular sections of the fabric ellipsoid, respectively. See the text for more explanation.

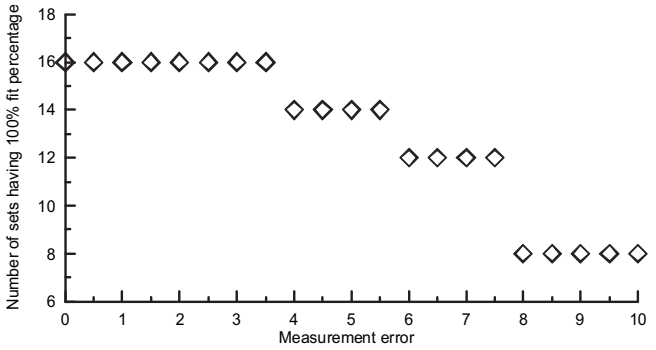

Fig. 4. The number of sets whose calculated fabric ellipsoids have a fit percentage of 100%. In this case where the primary set has four measurements, the total number of sets with a given measurement error is 16.

Table 2
Comparison between the fabric ellipsoids estimated by applying the Tocher's (1964) method and the above-proposed method, respectively, to three real sets from Lisle (1976). *V* is the acute angle between the long axis and one of the poles to the circular sections of the fabric ellipsoid. The fit percentage is the percent of sectional measurements that have an acute angle of less than 45° between the measured and the calculated traces.

Sets	Sections	Fabric traces	Methods	Fabric ellipsoid			Fit percentage
				Foliation	Lineation	*V*	
1	90/90	180/88	Tocher (1964)	55/88	143/34	72.5	100
	15/90	105/85					
	54/90	144/33	This paper	81/86	171/1	61.9	80
	144/90	54/85					
2	90/90	180/79	Tocher (1964)	Weak	121/67	≈0	100
	2/90	92/69					
	39/90	129/66	This paper	198/84	120/65	32.3	100
	126/90	36/90					
3	133/90	223/40	Tocher (1964)	263/62	178/11	50.5	100
	35/90	305/47					
	90/90	180/9	This paper	265/64	179/9	48.6	100
	181/90	271/64					

method. This makes us believe in the dependency of the four measurements in the set. In this example, the Tocher's method seems to have the advantage that it incorporates into graphical determination some empirical observations, based upon the spatial interrelationship among the measurements on the stereogram, that appears useful in reducing the range of the acceptable solutions.

6.2. Set two

There is some similarity and some difference between the fabric ellipsoids by Lisle (1976) and the proposed method, respectively, for this set. Both estimates have a similar lineation, but they have a different angle between the poles to the circular sections of the ellipsoid (Table 2). Actually, Lisle (1976) did not make the estimation using the Tocher's method but by visual appreciation, as he considered the unfavorable clustering around the origin of the traces. For the latter, the poles lie at the sides of each great circle that consists of the normal to the sectional plane and the trace on it, and the fit percentage is 100% (Fig. 5c–d). The latter result is therefore accepted with more confidence.

6.3. Set three

For this set, the fabric ellipsoids by the Tocher's method and the proposed method, respectively, match each other very well (Table 2). The good match is most likely attributed to the spread of data vectors that leads to a well-posed hyperplane in parameter space (Shan and Fry, 2006). This spreading can be evaluated from the distribution of eigen values of data matrix for the set (Table 3). The least second eigen value is close to the least third eigen value, and much larger than the least eigen value.

7. Discussion

As described above, Fresnel's theorem can explicitly be expressed in Eq. (11), from which we developed a new method for determining the fabric ellipsoid from independent sectional measurements.

7.1. Relationship between strain and stress analyses

Shan and Li (2008) recently compared the equation describing the sectional strain ellipse with the equation describing the Wallace-Bott hypothesis for a given fault/slip datum, and noted the similarity in formulation between them. This relationship becomes more apparent in this paper where Eq. (12) is directly comparable to Eq. (13). It further permits a simple transformation from sectional measurements of strain ellipses to fault/slip data, or from fault/slip data to sectional measurements of strain ellipses. For example, a sectional measurement of strain ellipse or $(s \quad p)$ is equivalent to a fault/slip datum or$(n \quad l)$. Such transformation is not one-to-one at all, because another fault/slip datum, whose normal to the fault plane is *l* and whose vector perpendicular to the slip line on the fault plane is *n*, or$(l \quad n)$, satisfies Eq. (13), too. It is however inappropriate to determinate in some way either the stress or the strain from a composite set of fault/slip data and sectional measurements of strain ellipses, as the relationship between the stress and the strain in rock is generally unknown.

7.2. Advantages and disadvantages

The nonlinear nature of Eq. (11) makes it difficult to solve for the two poles to the circular sections of the fabric ellipsoid, O_1 and O_2. However, instead of direct solution, we determine the fabric ellipsoid, according to Eq. (12), from which the locations of the poles are then calculated. This method is quite similar in formulation to Shan et al. (2008) method, although they are based upon different theories. Both provide an analytical solution of the fabric ellipsoid for a set of sectional measurements. Differently, nearly all of other pre-existing methods have a variety of numerical ways to restore the strain ellipsoid from strain ellipses measured on the different sections (e.g. Shimamoto and Ikeda, 1976; Oertel, 1978; Milton, 1980; Gendzwill and Stauffer, 1981; Owens, 1984; Shao and Wang, 1984; De Paor, 1990; Robin, 2002).

The method proposed in this paper has a major advantage over Tocher's method and probably other graphic methods in the applicability to any set of exposures, no matter how points O_1 and O_2 are located either at the two sides or at one side of plane *FS* or both on the stereogram. However, in the new method graphic construction is replaced by calculation. This may disappoint some of structural geologists who prefer visual presentation.

7.3. Measurement error

In Fig. 4, some of the sets start(s) to give an estimate with a fit percentage of less than 100%, when the measurement error becomes larger than 3.5°, a little larger in value than the precision of compass, commonly 2°. This turning point means a lot to structural geologists who measure the sectional planes and the fabric traces by compass, and estimate from them the fabric ellipsoid using the proposed method, the Tocher's (1964) method, or others. Besides, the measurement error may be caused by other

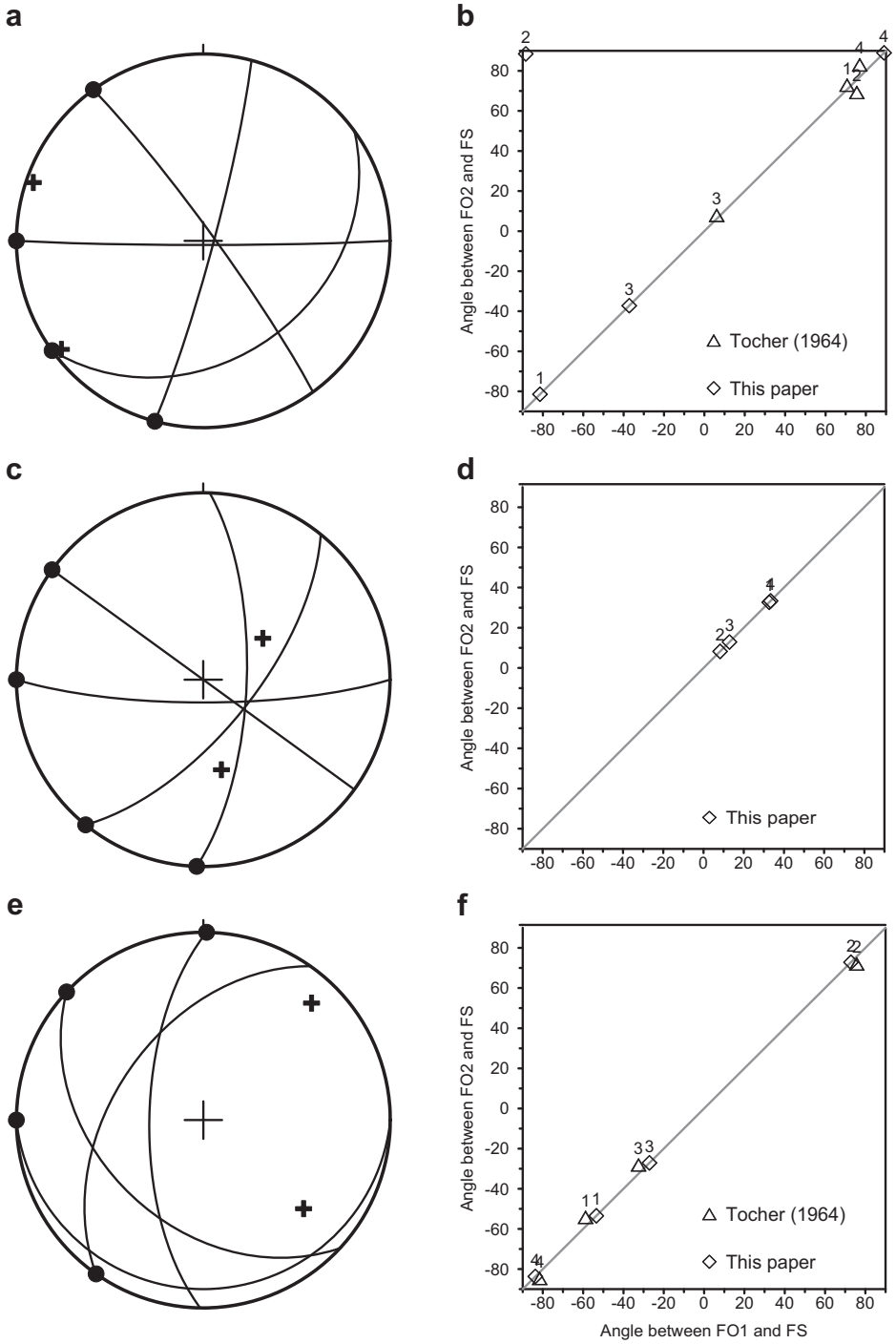

Fig. 5. Lower-hemisphere, equal-area projection of three real sets (Lisle, 1976; Table 2), and comparison between two angles, $\angle SFO_1$ and $\angle SFO_2$, for each individual measurement and the fabric ellipsoids obtained by the Tocher's (1964) method and the method proposed in this paper, respectively. In Fresnel's theorem, the two angles equal to each other. (a)–(b) are for set one, (c)–(d) for set two, and (e)–(f) for set three. See the caption of Fig. 3 for more explanation.

Table 3
The eigen values of data matrices for three real sets from Lisle (1976; Table 1).

Sets	Eigen values				
1	1.7527	1.3951	0.8426	0.0096	0.0000
2	2.2100	1.6875	0.0615	0.0410	0.0000
3	2.5478	0.8431	0.3805	0.2286	0.0000

possible factors including the smoothness of the sectional surface and the visibility of the fabric trace on the surface. It is thus likely at times that, in respect to the sectional plane the bearing of the fabric trace has a larger measurement error than the turning point. That is to say, in the case of only a minimal number of four measurements, there exists a possibility of having a highly inaccurate estimate, although it is small. A good remedy to this problem is to include more measurements as much as possible. Additionally, such inclusion tends to spread the measurements in parameter space,

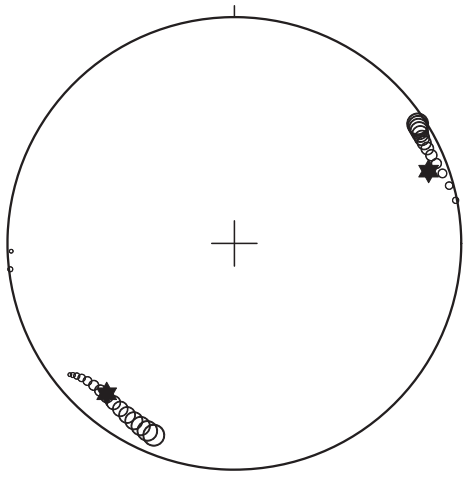

Fig. 6. The poles to the circular sections of the acceptable fabric ellipsoids, with a fit percentage of 100%, that result from a linear mixture of two eigen vectors in respect to the least and second least eigen values (Table 3). They are displayed as circles having a radius in proportion to the weight of the eigen vector in respect to the second least eigen value. They are looked for by use of a grid search in which the weight has a range of 0–1 in increments of 0.05. The symbol of filled stars represents the poles to the circular sections of the fabric ellipsoid by the Tocher's method (Table 2). Lower-hemisphere, equal-area projection.

which is favorable to the use of the proposed method in determining the fabric ellipsoid from them.

8. Conclusions

In optical crystallography (see Shubnikov, 1960, p.70), Fresnel's theorem describes how the extinction in any section is related to the circular sections of the optical indicatrix (Fig. 1a). This theorem is also applicable to fabric analysis and strain analysis due to the similarity in formulation between the optical indicatrix, the fabric ellipsoid and the strain ellipsoid (Lisle, 1976). It has an explicit expression in Eq. (11) in terms of the positions of the circular sections of the ellipsoid. As we prove, the expression is similar in formulation to the expression about the Wallace-Bott hypothesis for stress inversion. This highlights a simple relationship between strain analysis and stress analysis, as shown by Shan and Li (2008), and makes it possible to develop an analytical method, similar to the moment method by Fry (1999) and Shan et al. (2003), to determine the fabric ellipsoid from sectional measurements.

Artificial and real examples are taken to demonstrate the feasibility of the proposed method. In comparison with the Tocher's (1964) method that graphically determines the poles to the circular sections of the fabric ellipsoid, the proposed method is applicable to any set of exposures, no matter whether points O_1 and O_2 are located either at the two sides or at one side of plane *FS* or both on the stereogram.

A minimal number of four independent measurements are required in the determination. In the case of a set of four or a little more measurements, care needs be taken for two excuses, data dependency in relation to the limit of the exposures (Shan and Fry, 2006), and a small possibility of having a highly inaccurate fabric ellipsoid due to the measurement error.

Acknowledgment

This work is funded by National Basic Research Program of China 973 (Grant 2007CB411307), Hundred Talent Program of Chinese Academy of Sciences (KZCX0543081001), the National Key Project No. 2008ZX05008, and National Natural Science Foundation of China (Grant 40725009). R. J. Lisle helps check the written English of this paper. This paper is reviewed by T. G. Blenkinsop and K. Sarkarinejad who made valuable suggestions and modifications to it. This is contribution No. IS-1366 from GIGCAS.

Appendix

Proposition: The relative fabric ellipsoid may be defined as

$$\begin{bmatrix} 2o_{11}o_{21} & o_{11}o_{22}+o_{12}o_{21} & o_{11}o_{23}+o_{13}o_{21} \\ & 2o_{12}o_{22} & o_{12}o_{23}+o_{13}o_{22} \\ \text{symmetrical} & & 2o_{13}o_{23} \end{bmatrix} \tag{A1}$$

where O_1 and O_2 are the poles to the circular sections of the triaxial fabric ellipsoid. $O_1=[o_{11}\quad o_{12}\quad o_{13}]$ and $O_2=[o_{21}\quad o_{22}\quad o_{23}]$, where $o_{13}\geq 0$, $o_{23}\geq 0$.

Proof. Let us consider a special case where the axes of the fabric ellipsoid are along the coordinate axes. The *X*-, *Y*- and *Z*-coordinate axes are directed toward the east and the north, and upright, respectively. For a general case that does not show such parallelism, the present coordinate system may be rotated to meet this need, in advance. Accordingly, we have an expression of the absolute fabric ellipsoid in the coordinate system as follows,

$$\begin{bmatrix} \varepsilon_1^{-1} & 0 & 0 \\ 0 & \varepsilon_2^{-1} & 0 \\ 0 & 0 & \varepsilon_3^{-1} \end{bmatrix} \tag{A2}$$

where ε_1, ε_2, and ε_3 are the square of the lengths of the *X*-, *Y*- and *Z*-coordinate axes of the fabric ellipsoid, respectively. Matching the components of the above expressions leads to

$$o_{11}o_{22}+o_{12}o_{21}=0 \tag{A3}$$

$$o_{11}o_{23}+o_{13}o_{21}=0 \tag{A4}$$

$$o_{12}o_{23}+o_{13}o_{22}=0 \tag{A5}$$

$$2o_{11}o_{21}=k\varepsilon_1^{-1}-t \tag{A6}$$

$$2o_{12}o_{22}=k\varepsilon_2^{-1}-t \tag{A7}$$

$$2o_{13}o_{23}=k\varepsilon_3^{-1}-t \tag{A8}$$

where k and t are unknown constants that relate the relative fabric ellipsoid to the absolute fabric ellipsoid.

Eqs. (A3)–(A5) may be rewritten:

$$\frac{o_{11}}{o_{12}}=-\frac{o_{21}}{o_{22}} \tag{A9}$$

$$\frac{o_{11}}{o_{13}}=-\frac{o_{21}}{o_{23}} \tag{A10}$$

$$\frac{o_{12}}{o_{13}}=-\frac{o_{22}}{o_{23}} \tag{A11}$$

Multiplying the sides of the above equations gives,

$$\left(\frac{o_{11}}{o_{13}}\right)^2=-\left(\frac{o_{21}}{o_{23}}\right)^2 \tag{A12}$$

Similarly, we have

$$\left(\frac{o_{12}}{o_{13}}\right)^2=-\left(\frac{o_{22}}{o_{23}}\right)^2 \tag{A13}$$

$$\left(\frac{o_{13}}{o_{11}}\right)^2 = -\left(\frac{o_{23}}{o_{21}}\right)^2 \tag{A14}$$

Hence,

$$o_{11} = o_{21} = 0 \text{ for Eq. (A12)}, \tag{A15}$$

$$o_{12} = o_{22} = 0 \text{ for Eq. (A13)}, \tag{A16}$$

and

$$o_{13} = o_{23} = 0 \text{ for Eq. (A14)}. \tag{A17}$$

So far, simultaneously satisfying Eqs. (A3)–(A5) requires the existence of zero-value component(s) of vectors O_1 and O_2, either Eq. (A15) or Eq. (A16) or Eq. (A17). Because the points are located on the sphere with a unit-length radius, there exist only two possibilities that O_1 and O_2 have either one zero-value component or two zero-value components.

(1) One zero-value component

Suppose $o_{11} = o_{21} = 0$. Other suppositions lead to only a different state of the fabric ellipsoid, as may be shown below. Accordingly, from Eq. (A12) we know that $O_{12} = -O_{22}$, and $o_{13} = o_{23} > 0$. Substituting them into Eqs. (A6)–(A8),

$$0 = k\varepsilon_1^{-1} - t \tag{A18}$$

$$-2(o_{12})^2 = k\varepsilon_2^{-1} - t \tag{A19}$$

$$2(o_{13})^2 = k\varepsilon_3^{-1} - t \tag{A20}$$

Obviously, Eqs. (A18)–(A20) becomes valid if and only if

$$-k\varepsilon_2^{-1} - t \le 0, \text{and} \tag{A21}$$

$$k\varepsilon_3^{-1} - t \ge 0 \tag{A22}$$

These inequalities, as well as Eq. (A18) and the requirement of one zero-value component, give a fabric state of $k\varepsilon_3^{-1} > k\varepsilon_1^{-1} > k\varepsilon_2^{-1}$, or the triaxial ellipsoid. In this state, Eqs. (A13)–(A15) are solved for the positions of O_1 and O_2,

$$O_1 = \left[0 \quad \sqrt{\frac{\varepsilon_1^{-1} - \varepsilon_2^{-1}}{\varepsilon_3^{-1} - \varepsilon_2^{-1}}} \quad \sqrt{\frac{\varepsilon_3^{-1} - \varepsilon_1^{-1}}{\varepsilon_3^{-1} - \varepsilon_2^{-1}}}\right], \tag{A23}$$

and

$$O_2 = \left[0 \quad -\sqrt{\frac{\varepsilon_1^{-1} - \varepsilon_2^{-1}}{\varepsilon_3^{-1} - \varepsilon_2^{-1}}} \quad \sqrt{\frac{\varepsilon_3^{-1} - \varepsilon_1^{-1}}{\varepsilon_3^{-1} - \varepsilon_2^{-1}}}\right] \tag{A24}$$

For $k > 0$, it is fairly easy to know that vectors $O_1 + O_2$, $O_1 \times O_2$ and $O_1 - O_2$ are parallel to the long, intermediate and short axes of the fabric ellipsoid, respectively (Fig. A1a), and that

$$\tan^2 V = \left(\frac{o_{13}}{o_{12}}\right)^2 = \frac{\varepsilon_3^{-1} - \varepsilon_1^{-1}}{\varepsilon_1^{-1} - \varepsilon_2^{-1}} \tag{A25}$$

where V is the acute angle between either O_1 or O_2 and the long axis of the fabric ellipsoid.

For $k < 0$, $O_1 - O_2$, $O_1 \times O_2$ and $O_1 + O_2$ are parallel to the long, intermediate and short axes of the fabric ellipsoid, respectively (Fig. A1b), and

$$\tan^2 V = \left(\frac{o_{12}}{o_{13}}\right)^2 = \frac{\varepsilon_2^{-1} - \varepsilon_1^{-1}}{\varepsilon_1^{-1} - \varepsilon_3^{-1}} \tag{A26}$$

These features (see Lisle, 1976) demonstrate that the solutions in Eqs. (A23), (A24) are the locales of the poles to the circular sections of the ellipsoid, thus verifying the above proposition.

(2) Two zero-value components

Suppose $o_{11} = o_{21} = o_{12} = o_{22} = 0$. Accordingly, $o_{13} = o_{23} > 0$. Substituting these known components into Eqs. (A6)–(A8) gives

$$0 = k\varepsilon_1^{-1} - t \tag{A27}$$

$$0 = k\varepsilon_2^{-1} - t \tag{A28}$$

$$2(o_{13})^2 = k\varepsilon_3^{-1} - t \tag{A29}$$

Eq. (A29) is valid if and only if

$$k\varepsilon_3^{-1} - t \ge 0 \tag{A30}$$

This inequality, as well as Eqs. (A27), (A28) and the requirement of two zero-value components, gives a fabric state of $k\varepsilon_3^{-1} > k\varepsilon_1^{-1} = k\varepsilon_2^{-1}$. It is oblate for $(k < 0)$ or prolate for $k > 0$. In the state, both O_1 and O_2 have a similar orientation, and are parallel to the short $(k < 0)$ or the long $(k > 0)$ principal axes of the fabric ellipsoid. They are the solutions of the poles to the circular sections of the fabric ellipsoid, indeed.

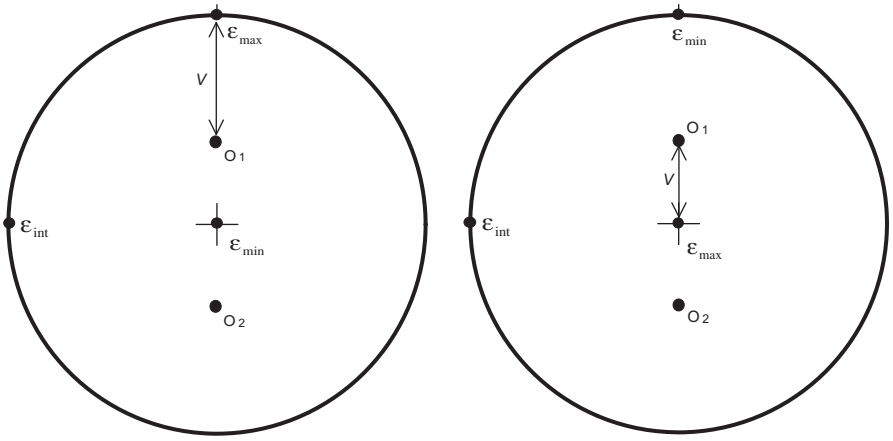

Fig. A1. The fabric state for $k > 0$ (a) and $k < 0$ (b), respectively. ε_{max},,ε_{int} and ε_{min} are the long, intermediate and short axes of the fabric ellipsoid. V is the acute angle between either O_1 or O_2 and the long axis of the fabric ellipsoid.

References

Bishop, A.W., 1966. The strength of soils as engineering materials. Ge'otechnique 16, 91–128.

Carey, M.E., Brunier, M.B., 1974. Analyse the' orique et nume'rique d'un mod-e'leme' canique e' le'mentaire applique' a l'e'tude d'une population de failles. Compte Rendus Hebdomadaires des Se'ances de l'Academie des Sciences 279, 891–894.

De Paor, D.G., 1990. Determination of the triaxial strain ellipsoid from sectional data. Journal of Structural Geology 12, 131–137.

Fry, N., 1999. Striated faults: visual appreciation of their constraint on possible palaeostress tensors. Journal of Structural Geology 21, 7–22.

Gendzwill, D.J., Stauffer, M.R., 1981. Analysis of triaxial ellipsoids; their shapes, plane sections, and plane projections. Mathematical Geology 13, 135–152.

Lanza, R., Meloni, A., 2006. The Earth's Magnetism: An Introduction for Geologists. Springer-Verlag, Berlin. 278pp.

Lisle, R.J., 1976. Some macroscopic methods of fabric analysis. Journal of Geology 84, 225–235.

Milton, N.J., 1980. Determination of the strain ellipsoid from measurements on any three sections. Tectonophysics 64, T19–T27.

Nemcok, M., Lisle, R.J., 1995. A stress inversion procedure for polyphase fault/slip data sets. Journal of Structural Geology 17, 1445–1453.

Oertel, G., 1978. Strain measurements from the measurement of pebble shapes. Tectonophysics 50, T1–T7.

Owens, W.H., 1984. The calculation of a best-fit ellipsoid from elliptical sections on arbitrarily orientated planes. Journal of Structural Geology 6, 571–578.

Ramsay, J.G., 1967. Folding and Fracturing of Rocks. McGraw-Hill, New York. 568pp.

Ramsay, J.G., Huber, M.I., 1983. The Techniques of Modern Structural Geology Volume 1: Strain Analysis. Academic Press, London. 307pp.

Robin, P.-Y.F., 2002. Determination of fabric and strain ellipsoids from measured sectional ellipses — theory. Journal of Structural Geology 24, 531–544.

Shan, Y., 2008. An analytical approach for determining strain ellipsoids from measurements on planar surfaces. Journal of Structural Geology 30, 539–546.

Shan, Y., Fry, N., 2006. The moment method used to infer stress from fault/slip data in sigma space: invalidity and modification. Journal of Structural Geology 28, 1208–1213.

Shan, Y., Gong, F.X., Li, Z., Lin, G., 2008. Determination of relative strain ellipsoids from sectional measurements of stretching lineation. Journal of Structural Geology 30, 682–686.

Shan, Y., Li, Z., 2008. Feasibility of graphic determination of stress from fault/slip data. Journal of Structural Geology 30, 739–745.

Shan, Y., Suen, H., Lin, G., 2003. Separation of polyphase fault/slip data: an objective-function algorithm based upon hard division. Journal of Structural Geology 25, 829–840.

Shao, J., Wang, C., 1984. Determination of strain ellipsoid according to twodimensional data on three or more intersection planes. Mathematical Geology 16, 823–833.

Shimamoto, T., Ikeda, Y., 1976. A simple algebraic method for strain estimation from ellipsoidal objects. Tectonophysics 36, 315–337.

Shubnikov, A.V., 1960. Principles of Optical Crystallography. Consultants Bur., New York. 186pp.

Tocher, F.E., 1964. Direct stereographic determination of the optic axes from a few extinction measurements: a progressive elimination technique. Mineralogy Magazine 33, 780–789.

Wheeler, J., 1989. A concise algebraic method for assessing strain in distributions of linear objects. Journal of Structural Geology 11, 1007–1010.

Zalohar, J., Vrabec, M., 2007. Paleostress analysis of heterogeneous fault-slip data: the Gauss method. Journal of Structural Geology 29, 1798–1810.